the FEBS Journal

Synthesis and evaluation of 1,4–naphthoquinone ether derivatives as *Sm*TGR inhibitors and new anti-schistosomal drugs

Laure Johann[1], Didier Belorgey[1], Hsin-Hung Huang[2], Latasha Day[2], Matthieu Chessé[1], Katja Becker[3], David L. Williams[2] and Elisabeth Davioud-Charvet[1]

1 UMR 7509, CNRS and University of Strasbourg, European School of Chemistry, Polymers and Materials, Strasbourg, France
2 Department of Immunology/Microbiology, Rush University Medical Center, Chicago, IL, USA
3 Biochemistry and Molecular Biology, Interdisciplinary Research Center, Justus Liebig University of Giessen, Germany

Keywords
flavoenzyme inhibitor; glutathione disulfide reductase; 1,4-naphthoquinone; *Schistosoma mansoni*; thioredoxin disulfide reductase

Correspondence
E. Davioud-Charvet, European School of Chemistry, Polymers and Materials, University of Strasbourg, UMR CNRS 7509, 25 Rue Becquerel, F-67087 Strasbourg, France
Fax: +33 368852742
Tel: +33 368852620
E-mail: elisabeth.davioud@unistra.fr

(Received 16 December 2014, revised 11 May 2015, accepted 18 June 2015)

doi:10.1111/febs.13359

Investigations regarding the chemistry and mechanism of action of 2-methyl-1,4-naphthoquinone (or menadione) derivatives revealed 3-phenoxymethyl menadiones as a novel anti-schistosomal chemical series. These newly synthesized compounds (**1**–**7**) and their difluoromethylmenadione counterparts (**8**, **9**) were found to be potent and specific inhibitors of *Schistosoma mansoni* thioredoxin-glutathione reductase (*Sm*TGR), which has been identified as a potential target for anti-schistosomal drugs. The compounds were also tested in enzymic assays using both human flavoenzymes, i.e. glutathione reductase (*h*GR) and selenium-dependent human thioredoxin reductase (*h*TrxR), to evaluate the specificity of the inhibition. Structure–activity relationships as well as physico- and electro-chemical studies showed a high potential for the 3-phenoxymethyl menadiones to inhibit *Sm*TGR selectively compared to *h*GR and *h*TrxR enzymes, in particular those bearing an α-fluorophenol methyl ether moiety, which improves anti-schistosomal action. Furthermore, the (substituted phenoxy)methyl menadione derivative (**7**) displayed time-dependent *Sm*TGR inactivation, correlating with unproductive NADPH-dependent redox cycling of *Sm*TGR, and potent anti-schistosomal action in worms cultured *ex vivo*. In contrast, the difluoromethylmenadione analog **9**, which inactivates *Sm*TGR through an irreversible non-consuming NADPH-dependent process, has little killing effect in worms cultured *ex vivo*. Despite *ex vivo* activity, none of the compounds tested was active *in vivo*, suggesting that the limited bioavailability may compromise compound activity. Therefore, future studies will be directed toward improving pharmacokinetic properties and bioavailability.

Introduction

Schistosomiasis, also called bilharzia after its discovery by Theodor Bilharz [1], is a widespread tropical disease caused by the helminth parasites of the genus *Schistosoma*, including *S. mansoni* [2]. It is a devastating tropical disease, ranking second after malaria in terms of social and economic impact and public health importance and affecting more than 200 million people worldwide [3,4]. No vaccine is available, and the only available drug, praziquantel, is used extensively, currently being administered to more than 10 million

Abbreviations
DTNB, 5,5′-dithiobis-(2-nitrobenzoic acid); GSH, glutathione; (*h*)GR, (human) glutathione reductase; (*h*)TrxR, (human) thioredoxin reductase; (*Sm*)TGR, (*Schistosoma mansoni*) thioredoxin-glutathione reductase.

people annually [5,6]. No new drugs have been introduced since praziquantel, and previous drugs are no longer produced or are not effective against all species of *Schistosoma* parasites [7]. As it is likely that praziquantel-resistant/tolerant parasites will develop [8], there is an urgent need to find new anti-schistosomal drugs.

Adult *S. mansoni* worms live in the mesenteric veins of their human hosts, where they may survive for up to 30 years [9]. Because they reside in an aerobic environment, they must have effective mechanisms to maintain their cellular redox balance. Furthermore, worms must be able to reduce reactive oxygen species generated by the host's immune response. In most eukaryotes, there are two major systems based on NADPH-dependent flavoenzymes that regenerate thiols from disulfide substrates and detoxify reactive oxygen species: one is based on the tripeptide glutathione (GSH) and glutathione reductase (GR, EC 1.8.1.7) and the other based on thioredoxin and thioredoxin reductase (TrxR, EC 1.8.1.9). These two enzymes are absent in *S. mansoni*, and are replaced by a unique bifunctional seleno-enzyme, thioredoxin–glutathione reductase (*Sm*TGR, EC 1.8.1.9) [10]. This enzyme plays a crucial role in *S. mansoni* thiol redox metabolism, and has been identified as a key drug target [11]. The aim of this study was to identify a new lead anti-schistosomal chemical series, and to design novel inhibitors of this essential enzyme.

A preliminary inhibitor screen led to identification of the (substituted phenoxy)methyl menadione derivative **1** (Fig. 1) with a carboxylic acid function as a potent *Sm*TGR inhibitor with inhibitory activity in the nanomolar range. However, compound **1** was only able to kill cultured adult worms at relatively high concentrations (50 μM). Because of this limited activity, which is probably due to the known limited membrane permeability of carboxylic acids, a series of new menadione derivatives bearing lipophilic moieties or fluorinated groups on the oxyphenylmethylene arm were synthesized to improve the pharmacological profile. These compounds were tested by both enzyme and biological assays to identify potential new anti-schistosomal agents.

Results and Discussion

Chemistry

A new series of (substituted phenoxy)methyl menadione derivatives was synthesized based on the structure of **1** (Fig. 1). The 2,6-difluorophenol group is a known bioisostere of the carboxylic acid function [12]. The introduction of bioisosteric moieties of the carboxylic acid may improve the pharmacokinetic profiles of the inhibitors [13]. Furthermore, compounds were generated to allow introduction of fluorine groups in order to enhance the lipophilicity [14] and cell permeability of the compounds. A synthetic route for preparation of the chemical series was investigated that allowed preparation of new bioisosteric analogs and pro-drugs with optimized inhibition and pharmacokinetic profiles. Based on the structure of the potent *Sm*TGR inhibitor (**1**) the benzoic acid group was replaced with a benzonitrile group (**2**) or a difluoromethoxyphenol group (**3**), which are known to enhance the cellular permeability of the parent benzoic acid, or was changed upon introduction of halogen groups, e.g. chloro (**4**), bromo (**5**) or CF_3 (**6**, **7**) groups (Fig. 1).

From the synthetic point of view, the (substituted phenoxy)methyl menadione derivative **2**, bearing a cyano group instead of the benzoic acid function found in **1**, was obtained with 13% overall yield from commercially available 4-cyanophenol (Fig. 2A). Compound **2** may be considered a pro-drug of **1**. The side chain of 4-cyanophenol was elongated by reaction with ethylchloroacetate under basic conditions to create **2c** as white crystals with 97% yield. The ethyl ester was then saponified to give the acid **2d** with 65% yield. Menadione was then alkylated through the radical decarboxylation of acid **2d** under Kochi–Anderson

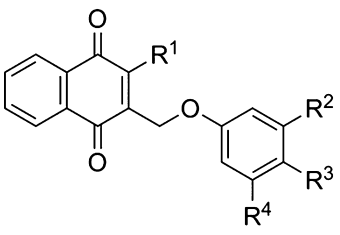

1 R^1= Me; R^2, R^4= H; R^3= COOH
2 R^1= Me; R^2, R^4= H; R^3= CN
3 R^1= Me; R^2, R^4= F; R^3= OMe
4 R^1= Me; R^2, R^4= H; R^3= Cl
5 R^1= Me; R^2, R^4= H; R^3= Br
6 R^1= Me; R^2, R^3= H; R^4= CF_3
7 R^1= Me; R^2=H; R^3= OMe; R^4= CF_3
8 R^1= CHF_2; R^2, R^4= H; R^3= CN
9 R^1= CHF_2; R^2=H; R^3= OMe; R^4= CF_3

Fig. 1. Structures of the 3-phenoxymethyl menadione derivatives.

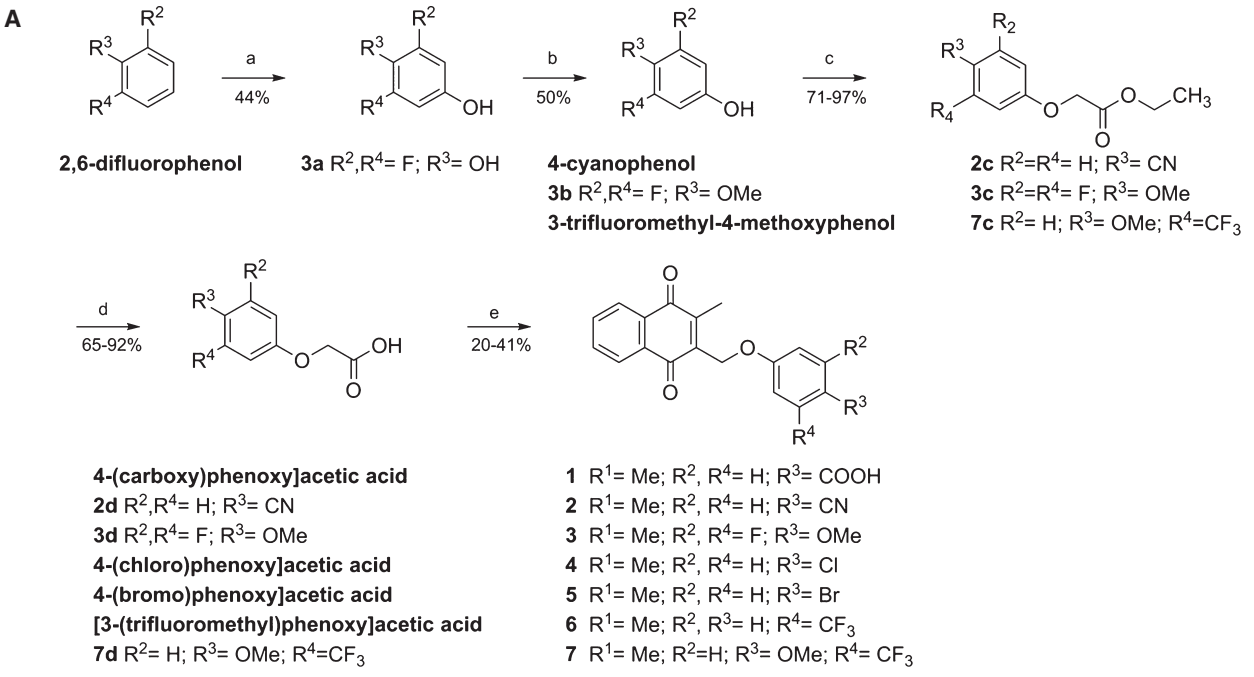

Reagents and conditions: a) 1. $K_2S_2O_8$, NaOH; 2. HCl; b) K_2CO_3, Me_2SO_4, acetone, RT, 1 day; c) $ClCH_2COOEt$, NaI, K_2CO_3, reflux, 4 h; d) 1. NaOH 10%, reflux, 2 h; 2. HCl or 10% NaOH in MeOH, reflux, 5 h; e) menadione, $AgNO_3$, $(NH_4)_2S_2O_8$, 85°C, 3 h.

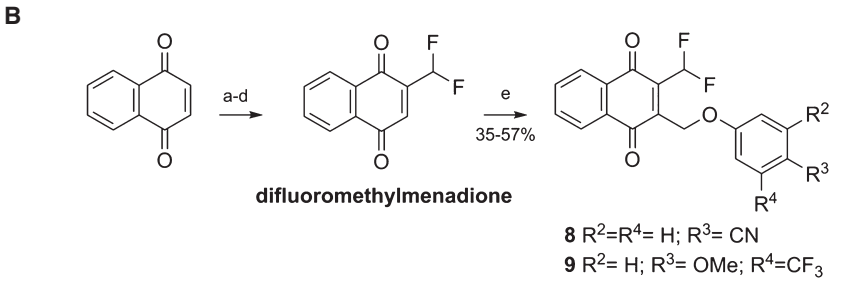

Reagents and conditions: a-d) synthesis described in Ref. [17]; e) phenoxyacetic acid **2d** for compound **8**, or **7d** for compound **9**, $AgNO_3$, $(NH_4)_2S_2O_8$, 85°C, 3 h.

Fig. 2. Synthesis of 3-phenoxymethylmenadione derivatives (A) and 2-difluoromethyl analogs (B).

conditions [15] to obtain the final (*p*-cyanophenoxy) methyl menadione derivative (**2**) with 21% yield. Starting from the commercially available difluorophenol, the (difluorophenoxy)methyl menadione derivative **3** was obtained with an overall yield of 5% (Fig. 2, route A). The hydroquinone **3a** was obtained through Elbs oxidation [16] with a yield of 44% and was then submitted to selective methylation with dimethylsulfate under mild basic conditions to give the 4-methoxy-3,5-difluorophenol (**3b**) with 50% yield. The side chain of the phenol **3b** was elongated by reacting with ethylchloroacetate under basic conditions to produce the ester **3c** with 71% yield. Saponification of **3c** led to the carboxylic acid **3d** with a yield of 77%. The acid **3d** was subjected to Kochi–Anderson radical decarboxylation to obtain the final difluorophenol methoxy ether derivative (**3**) with 41% yield. To introduce more structural diversity into the (substituted phenoxy) methyl menadione series, other analogs were synthesized such as molecules bearing various halogens. Addition of halogen increases the lipophilicity of the compounds, changes their redox potential value, and improves their metabolic stability in the host. Commercially available 2-(4-chlorophenoxy)acetic acid and

2-(4-bromophenoxy)acetic acid were allowed to react with menadione via Kochi–Anderson radical decarboxylation to produce the corresponding 3-phenoxymenadione derivatives, **4** and **5**, with 35% and 24% yield, respectively.

Finally, another series of compounds was investigated in which fluorine was introduced directly onto the methyl group of the menadione core (Fig. 2, route B). Commercially available 1,4-naphthoquinone was reduced using $SnCl_2$/HCl, and the resulting dihydronaphthoquinone was methylated by dimethylsulfate under mild basic conditions. The dimethoxynaphthalene intermediate was then successively formylated (98% yield) and treated with 2.0 equivalents of diethylaminosulfur trifluoride to obtain 2-(difluoromethyl)-1,4-dimethoxynaphthalene with a yield of 92%, as described previously [17]. Subsequent oxidation with cerium ammonium nitrate produced the difluorinated menadione with 93% yield. The difluoromethylmenadione derivative and the *p*-cyanophenylacetic acid were subjected to Kochi–Anderson radical decarboxylation to produce difluoromethylmenadione derivatives with an oxyphenylmethylene arm, i.e. the 3-[(4-cyanophenoxy)methyl] derivative **8** (with 35% yield) and the 3-[(4-methoxy-3-(trifluoromethyl) phenoxy)methyl] derivative **9** (with 57% yield).

Electrochemistry

The redox potentials of the various (substituted phenoxy)methyl menadione derivatives were determined by cyclic voltammetry in dimethylsulfoxide (DMSO) containing 0.1 M tetra-*n*–butylammonium hexafluorophosphate as the electrolyte system. The results obtained using the 1,4–naphthoquinones **1**, **2**, **5**, **7**, **8** and **9**, are shown in Table 1. For all the compounds, a $1e^-$ quasi-reversible redox wave attributed to the monoradical anion may be observed (ΔE_p of approximately 96–170). The quasi-reversibility of this electron transfer process is indicated by the large ΔE_p separation (a theoretical ΔE_p of 60 mV is expected for an ideal $1e^-$ transfer) as well as an I_{pc1}/I_{pa1} ratio significantly greater than 1. A second quasi-reversible redox wave may be observed for **2** (Table 1) and **7**, which is not fully reversible, with $\Delta E_p < 70$ mV. However, we estimated the half-wave potential $E^2_{1/2}$ as well as the $\Delta E_{1/2}$ separation ($E^1_{1/2} - E^2_{1/2}$), and these were found to be comparable to each other. For compounds **1** and **5**, the second electron transfer affording the quinone dianion appears to be an irreversible process, thus precluding determination of the half-wave potential. This electrochemical behavior may result from either comproportionation reactions or fast and irreversible dimerization between the quinone dianion (NQ^{2-}) and the naphthoquinone (NQ) to afford an electro-inactive dimeric species NQ_2^{2-}. When the methyl of the menadione core was replaced by CHF_2 in **2** and **7**, there was no second redox wave, and the $1e^-$ reduction potential showed a significant anodic shift of 200 mV with respect to the CH_3-substituted analog (Table 1). This feature clearly reflects the highly oxidant character of compounds **8** (Table 1) and **9**, as previously observed for fluoromethyl menadione analogs [17–19], and therefore their greatest reactivity.

Physico-biochemistry of glutathionylation

Absorption spectrophotometry was used to estimate the pK_a value of the difluoromenadione derivative **9** (Fig. 3A). Significant spectral variation and color change of compound **9** were observed when the pH was increased from acidic (below pH 7, colorless solution) to basic conditions (pale yellow solution, pH approximately 11.5–12). These observations clearly indicate that, due to the fluorine atoms, deprotonation of the difluoromenadione species may occur in a biocompatible pH window. Statistical processing of the data resulted in a single pK_a value of approximately 7.1 ± 0.5 (Fig. 3B).

Using absorption spectrophotometry, we then investigated the glutathionylation reaction kinetics of three difluoromenadione species: the difluoromenadione itself (Fig. S1) and both difluoromethylmenadione derivatives bearing an oxyphenylmethylene arm, i.e. compound **8** (Fig. S2) and compound **9** (Fig. 3C–F). Taking into account the estimated acido-basic properties, it may be anticipated that a mixture of protonated difluoromenadione and deprotonated derivatives dominates under our experimental conditions. Figure S1 shows the absorption changes for a 0.2 mM of difluoromethylmenadione solution over the course of glutathionylation following addition of five equivalents of GSH (1 mM final). The spectral window used (300–500 nm) allowed monitoring of the weak n–π* transitions of the quinone moiety. Interestingly, glutathionylation induces formation of an intense absorption band in the visible region (approximately 440 nm), which allowed the reaction to be monitored easily. Biphasic kinetic behavior was observed (Fig. S1A,B). Statistical tools were used to process the spectral and kinetic data, and to calculate pseudo-first-order rate constants for the two-step process as well as electronic spectra of the kinetic intermediate (P1) and the final product P2 (Table 2). These spectral observations may be rationalized as formation of the quinone methide (kinetic intermediate P1) prior to a Michael

Table 1. Electrochemical data for 3-phenoxymethylmenadione derivatives measured using cyclic voltammetry [DMSO; I = 0.1 M tetra-*n*-butylammonium hexafluorophosphate, $E_{1/2}$ (V) = (E_{pc} + E_{pa})/2; ΔE (mV) = E_{pa} − E_{pc}; $\Delta E_{1/2}$ (V) = $E^1_{1/2}$ − $E^2_{1/2}$. v = 200 mV s^{-1}; reference electrode = KCl (3 M)/Ag/AgCl; working electrode = glassy carbon disk of 0.07 cm^2 area; auxiliary electrode = Pt wire]. Cyclic voltammograms of the 3-phenoxymethylmenadione representatives [the menadione **2** (black bold line) and its difluoromethyl analog **8** (red dashed line)] were recorded using a platinum electrode in $CHCl_2$ with 0.1 M tetra-*n*-butylammonium tetrafluoroborate as the supporting electrolyte at a 200 mV s^{-1} scan rate.

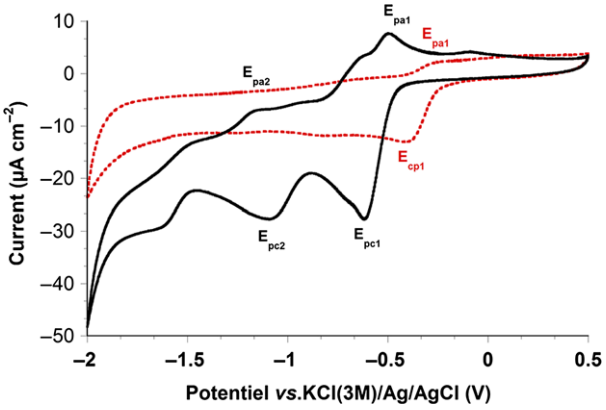

	E_{pc1} (V)	E_{pa1} (V)	I_{pc1}/I_{pa1}	$E^1_{1/2}$ (V)	ΔE_p (mV)	E_{pc2} (V)	E_{pa2} (V)	I_{pc2}/I_{pa2}	$E^2_{1/2}$ (V)	ΔE_p (mV)	$\Delta E_{1/2}$ (mV)
1	−0.628	−0.532	1.27	−0.580	96	−1.265	IRR	IRR	IRR	IRR	NA
2	−0.620	−0.492	2.29	−0.556	128	−1.154	−1.100	2	−1.127	54	571
5	−0.627	−0.508	1.89	−0.508	119	−1.158	IRR	IRR	IRR	IRR	NA
7	−0.620	−0.506	2.92	−0.563	114	−1.132	−1.120	1.75	−1.126	12	563
8	−0.414	−0.244	3.31	−0.329	170	ND	ND	ND	ND	ND	ND
9	−0.326	−0.215	1.67	−0.271	111	ND	ND	ND	ND	ND	ND

IRR, irreversible reduction; NA, not applicable; ND, no second wave was observed.

addition of glutathione and concomitant fluorine elimination (concerted mechanism, product P2). However, as previously reported, both the structure and reactivity of difluoroquinone methides may be compared to those of related β-fluorocarbanions that are known to generate further additions with nucleophiles and to cross- or self-polymerize (Table 2) [19]. The same kinetic approach was used for the compounds **8** and **9**, which share common spectral behavior upon addition of GSH at pH 7.5 (Fig. S2 and Fig. 3, respectively). The n–π* transitions show a significant hyperchromic shift upon addition of GSH and allowed monitoring of the glutathionylation kinetics of these two phenoxymethyl-substituted difluoromenadiones. Similarly to difluoromenadione, a biphasic kinetic process was observed. Interestingly, the three compounds examined in this work are characterized by a common fast kinetic step, as deduced from their comparable k_1 values (Table 2) and electronic spectra (Fig. 3F, and Figs S1C and S2C). This suggests that the three compounds experience the same reaction (i.e. deprotonation and addition/elimination), leading to the reactive quinone methide intermediate P1, and then the GSH conjugates P2 and other products. As previously discussed [17,19], the difluoromenadione core via the quinone methide is highly reactive towards nucleophiles; it acts as a difluoroacrolein that is prone to polymerization (Table 2). However, the kinetics of adding GSH are greatly influenced by the substitution pattern of the difluoromenadione core, as indicated by the almost tenfold decrease in the k_2 values measured for both compounds **8** and **9** compared to the difluoromenadione itself. However, no distinct behavior was observed between the two phenoxymethyl-substituted compounds **8** and **9**.

Glutathionylation reactions and LC-MS analyses of reaction mixtures containing difluoromethylmenadione–GSH conjugates

The spontaneous reaction of difluoromethylmenadione with free reduced GSH gave rise to a complex mixture due to the reactions occurring at various sites of the electrophile (Fig. S3). The first step for quantifying the potential glutathione adducts was to develop a chromatographic method to resolve the conjugates, which were detected using positive ESI-MS techniques.

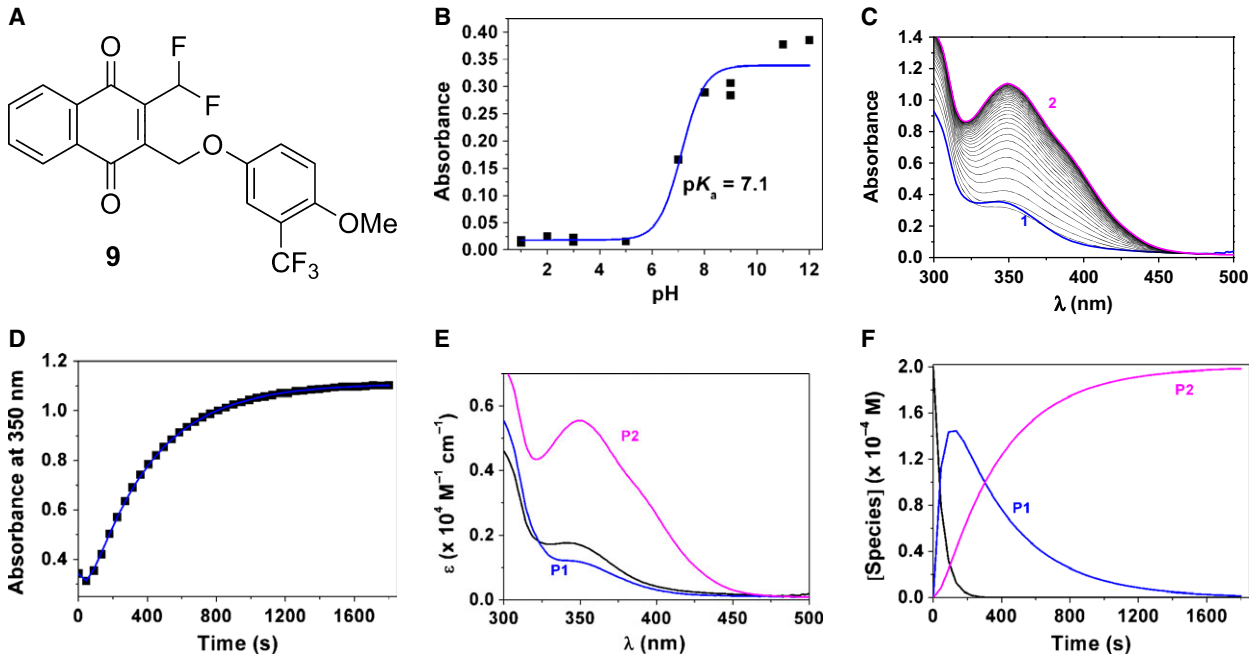

Fig. 3. (A) Structure of the 3-[(4-methoxy-3-(trifluoromethyl) phenoxy)methyl] difluoromethylmenadione derivative **9**. (B) Determination of the pK_a value for the difluoromethylmenadione derivative **9**. (C–F) Changes in the absorption spectra for **9** upon glutathione addition. (C) Absorption spectrophotometric variation and (D) absorbance at 350 nm measured over the time course of the glutathionylation reaction with the difluoromethylmenadione derivative **9**. Solvent: 200 μL acetonitrile + 265 μL NH_4OH buffer at pH 7.5; concentration of **9** = 2×10^{-4} M (10 μL stock at 10 mM); concentration of GSH = 10^{-3} M (25 μL stock at 20 mM); T = 25 °C. (1) t = 0 s; (2) t = 1800 s. (E) Electronic absorption spectra measured for the difluoromethylmenadione derivative **9**, its fluoro quinone methide (P1) intermediate, and its glutathione adducts (P2), and (F) distribution diagram for the difluoromethylmenadione derivative **9** and its products (P1 and P2) as a function of time. Solvent: 200 μL acetonitrile + 265 μL NH_4OH buffer at pH 7.5; concentration of **9** = 2×10^{-4} M (10 μL stock at 10 mM); concentration of GSH = 10^{-3} M (25 μL stock at 20 mM); T = 25 °C.

As shown in Fig. S3, the LC-MS chromatogram contains a number of peaks due to the presence of several expected diastereo- and regioisomers formed by reaction with GSH at the difluoroquinone methide or at C3 of the quinone core. All difluoromethylmenadione–GSH conjugates showed the same pattern in the LC-MS traces (Fig. S3), and all mono- and di-GSH conjugates were detected (Table S1).

Biological activities

*Sm*TGR inhibitory activity

The library of representative (substituted phenoxy) methyl menadione derivatives was tested for inhibitory activity using the 5,5′–dithiobis-(2–nitrobenzoic acid) (DTNB) assay (Table 3). All compounds inhibited *Sm*TGR activity with IC_{50} values in the nanomolar range (**1**, 482 nM; **2**, 462 nM; **3**, 407 nM; **4**, 457 nM; **5**, 784 nM), indicating excellent recognition of the menadione-anchored oxyphenylmethylene arm by *Sm*TGR. Interestingly, the most potent *Sm*TGR inhibitors were the difluoromenadione derivatives **8** and **9**, whose difluoromenadione core [17] has been shown to act as a suicide substrate for related flavoenzymes, namely GRs from human and *Plasmodium falciparum* [17]. Similar results were found with mono- [18] or tri- [19] fluoromenadione cores, which demonstrate fast irreversible inhibition of both flavoenzymes. These results validate our finding that the difluoromenadione core is a suicide substrate of the parasitic *Sm*TGR.

Time-dependent inactivation of *Schistosoma mansoni* TGR activity

Time-dependent inactivation of *Sm*TGR was studied using the DTNB reduction assay to evaluate the residual activity of the reacted enzyme (Table 3). A pair of menadione/difluoromethylmenadione derivatives, compound **7** and compound **9**, was selected on the basis of inhibition potency. Upon pre-incubation with NADPH and the inhibitor for 0, 2.5, 5 and 10 min, inactivation of *Sm*TGR by **7** at low concentration (≤ 3 μm) was shown to follow pseudo-first-order reaction kinetics (Fig. 4A). The experimental data allowed application

Table 2. Proposed chemical reactivity of difluoromethylmenadiones and rate constants for formation of difluoro-based quinone methide (P1) and glutathione adducts (P2).

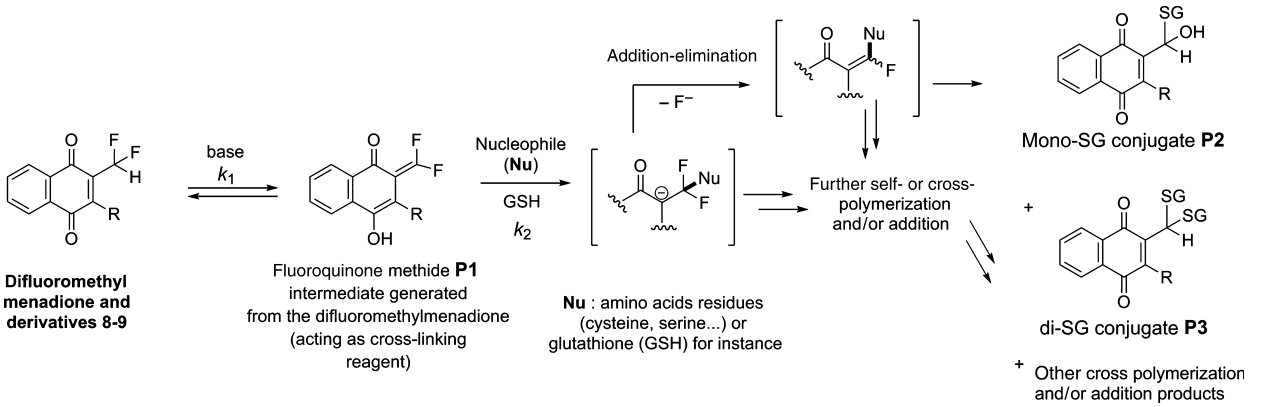

	k_1 (s^{-1})	k_2 (s^{-1})
Difluoromethylmenadione	2.13×10^{-2}	1.57×10^{-2}
Compound **8**	3.22×10^{-2}	3.52×10^{-3}
Compound **9**	2.04×10^{-2}	2.76×10^{-3}

of the derivation by Kitz and Wilson [20] for irreversible inactivation. A semi-logarithmic plot of the fraction of non-inhibited enzyme activity $\ln(v_i/v_0)$ versus incubation time yielded straight lines with increasing slopes at short time periods, equivalent to the apparent rate constant of irreversible inhibition (k_{obs}). A secondary plot expressing k_{obs} as a function of inhibitor concentration followed the equation:

$$k_{obs} = (k_i \times [I])/(K_I + [I]) \quad (1)$$

where K_I represents the dissociation constant of the inhibitor, and k_i is the first-order rate constant for irreversible inactivation, respectively. A hyperbolic curve at low inhibitor concentration allowed estimation of k_i as 0.57 ± 0.02 min^{-1}, and K_I as 0.8 ± 0.08 μm, and of the second-order rate constant k_i/K_I as 1.18×103 $m^{-1} \cdot s^{-1}$ (Fig. 4B). The resulting half-time value ($t_{1/2}$) of inactivation of *Sm*TGR was determined to be 1.29 min. The results are consistent with our concept of mechanism-based inhibition by menadione derivatives acting as NADPH-consuming redox cyclers (Fig. 5, pathway A), resulting in dead-end enzymes, as previously discussed [13,17–19,21,22].

In the case of the difluoromethyl analog **9**, inactivation of *Sm*TGR was evaluated using pre-incubation times of 0 and 5 min in the presence or absence of NADPH. At low inhibitor concentrations, an NADPH-dependent and time-dependent inhibition was observed at very low inhibitor concentration (data not shown), as observed for a monofluoromethyl naphthoquinone derivative inactivating *h*GR [18], and the dissociation and first-order rate constants for irreversible inactivation were determined to be $K_I = 0.26 \pm 0.17$ μm and $k_i = 0.64 \pm 0.12$ min^{-1}, respectively. In this mechanism, NADPH-dependent reduction of the napthoquinone is faster than proton subtraction of the difluoromethyl group. At high inhibitor concentrations, in contrast to the NADPH-dependent, TGR-catalyzed activation observed at low concentrations, incubation of the enzyme with compound **9** in the absence of NADPH resulted in inactivation (Fig. 4C), suggesting that the difluoromethylmenadione derivative **9** followed two possible pathways. This observation may be rationalized as follows: the low pK_a value of the difluoromethyl group, determined to be approximately 7.1, implies that proton subtraction quickly occurred at physiological pH and dominates (Fig. 5, pathway B), mainly prior to the enzymic reduction, and the highly reactive difluoroquinone methide intermediate (P1) is likely to act as a cross-linking reagent, by analogy to the difluoro acrolein analog in polyacrolein formation, or the *gem*-difluoroalkenes, which are known to be exclusively attacked by nucleophiles at the *gem*-difluoromethylene carbon atoms to form β-fluorocarbanions [17,23] Further additions to the carbanions may lead to insoluble cross-linked protein (polymers). However, elucidation of the structure of the cross-linked protein is extremely difficult due to their lack of stability and solubility. In attempts to co-crystallize *Sm*TGR with the difluoromethylmenadione analog **8**, fast precipitation of an inactivated insoluble *Sm*TGR enzyme after reaction with **8** was observed upon polyalkylation or cross-linking reactions (data not

Table 3. *In vitro* inhibition of *Sm*TGR and related human disulfide reductases *h*GR and *h*TrxR.

Compound	R^1	R^2	IC_{50} (nM) (*Sm*TGR assay)[a]	IC_{50} (nM) (*h*GR assay)[b]	IC_{50} (nM) *h*TrxR assays		
					Wild-type placental *h*TrxR		Sec498C TrxR
					Trx assay[c]	DTNB assay[d]	DTNB assay[d]
1	Me	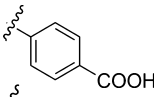	482	2300	2000	3000	40 000
2	Me	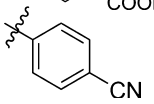	462	8500	1500	1200	6000
3	Me	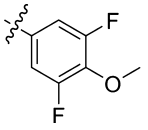	407	>25 000	2000	2000	>100 000
4	Me	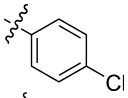	457	5500	700	700	>100 000
5	Me	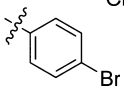	784	>5000	800	800	>100 000
6	Me	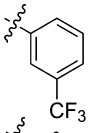	166	600	3000	1500	>50 000
7	Me	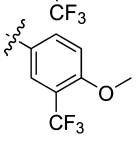	200	12 000	800	1500	>50 000
8	CHF_2	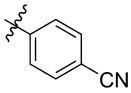	144	2100	13	14	370
9	CHF_2	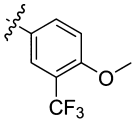	46	–	–	–	–
Potassium antimonyl tartrate[a]		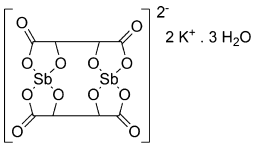	173	–	–	–	–

[a] The values were determined at pH 7 and 25 °C in the presence of 100 μM NADPH, 3 mM DTNB. Potassium antimonyl tartrate was used as a drug reference.

[b] The values were determined at pH 6.9 and 25 °C in the presence of 100 μM NADPH, 1 mM glutathione disulfide.

[c] The values were determined at pH 7.4 and 25 °C in the presence of 100 μM NADPH and 20 μM *h*TrxC72S after 10 min pre-incubation [28].

[d] The values were determined at pH 7.4 and 25 °C in the presence of 200 μM NADPH and 3 mM DTNB after 10 min pre-incubation [28].

shown). It is noteworthy that inhibitor concentration-dependent flavoenzyme inactivation was previously observed with mono- and difluoromethyl menadione derivatives in inactivation studies of human and *Plasmodium falciparum* GRs [18,19]. Consequently, NADPH-dependent reduction of difluoromethylmenadione derivatives is not a prerequisite for *Sm*TGR inactivation via pathway B, and the precipitated cross-linked inactive *Sm*TGR did not enter continuous NADPH-dependent redox cycling.

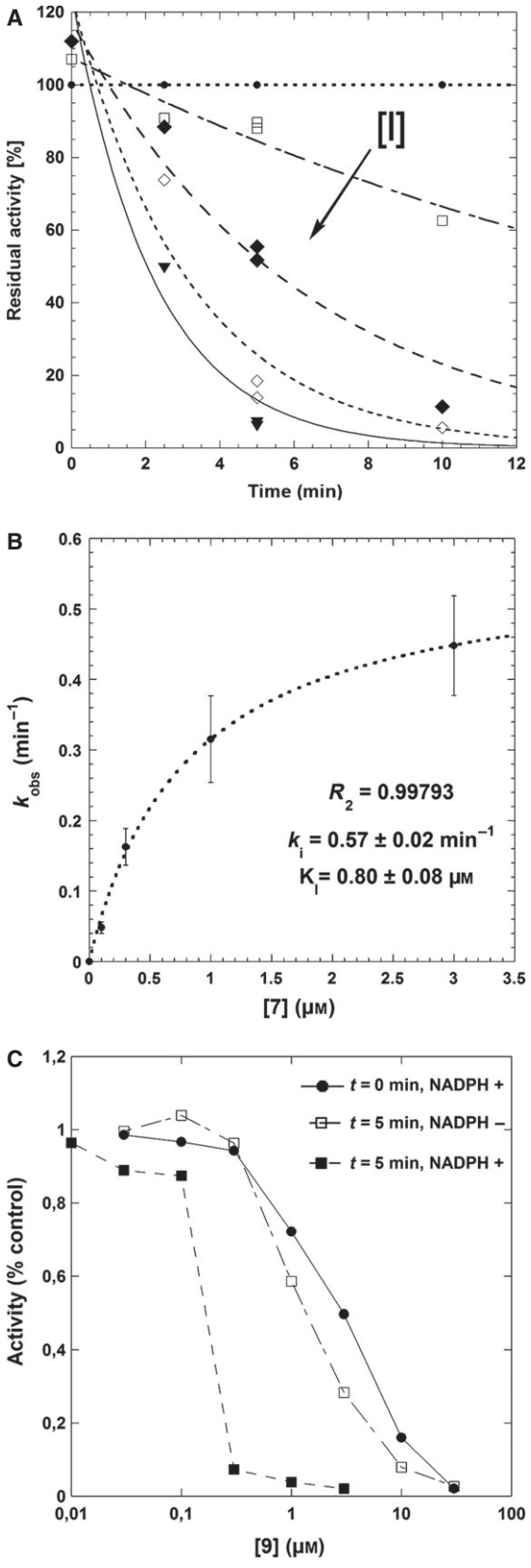

Fig. 4. Time-dependent inactivation of *Schistosoma mansoni* thioredoxin-glutathione reductase by compound **7** (A,B) and compound **9** (C). (A,B) *Sm*TGR (40 nM in 100 μL) was incubated in the presence of 100 μM NADPH and various inhibitor concentrations at 25 °C for various incubation periods (0, 2.5, 5 and 10 min). In (A), the concentrations of compound **7** used were 0 μM (closed circles), 0.1 μM (open squares), 0.3 μM (closed diamonds), 1.0 μM (open diamonds), and 3.0 μM (closed triangles). In (B), the k_{obs} data versus [I] were fitted to Eqn 1 (see text), which resulted in the hyperbolic curve (dashed line). At low inhibitor concentration, the dissociation constant and the first-order rate constant for irreversible inactivation were determined to be $K_I = 0.8 \pm 0.08$ μM and $k_i = 0.57 \pm 0.02$ min^{-1}, respectively. (C) *Sm*TGR (40 nM in 100 μL) was incubated in the presence of 100 μM NADPH and inhibitor at varying concentrations (0, 0.03, 0.1, 0.3, 1.0, 3.0, 10.0 and 30.0 μM) for 0 min (closed circles) and 5 min (closed squares). Reactions were also performed with the pre-incubated enzyme in the absence of NADPH for 5 min (open squares). Then 5 μL aliquots were removed, and the remaining activity was measured using a standard DTNB reduction assay as described in Experimental procedures. DMSO (3.4% final concentration) was present in all incubation mixtures.

*h*GR inhibitory and *h*TrxR inhibitory activity

Examination of the activity of these novel small molecules against human disulfide reductase 'orthologs' demonstrated an impressive degree of selectivity for *Sm*TGR inhibition compared to other human flavoenzymes. To assess the specificity of the molecules inhibiting *Sm*TGR, the library was also tested for inhibitory activity against *h*GR. With the exception of **6** (600 nM) and in contrast to the results with *Sm*TGR, none of the tested compounds were inhibitors of *h*GR in the nanomolar range. Their inhibitory activity is at least fivefold lower based on IC_{50} values. The library was also tested against *h*TrxR. Two assays were performed: the thioredoxin assay and the DTNB assay (see Experimental procedures). The results were comparable for the two methods (Table 3). For the majority of compounds, the IC_{50} values were in the micromolar or high nanomolar range (**1**, 2–3 μM; **2**, 1.2–1.5 μM; **3**, 2 μM; **4**, 0.7 μM; **5**, 0.8 μM; **6**, 1.5–3 μM; **7**, 0.8–1.5 μM). In particular, the IC_{50} for **6** was approximately tenfold higher for *h*TrxR than for *Sm*TGR, and that for **7** was approximately fivefold higher. A notable exception was **8**, the most potent inhibitor of *Sm*TGR, which is also a very potent inhibitor of *h*TrxR (IC_{50} = 13–14 nM) but a weak inhibitor of *h*GR (IC_{50} = 2.1 μM).

In vitro cytotoxicity against *S. mansoni* worms and human cells

All compounds were tested at 50 μM (Fig. 6) for a period of 4 days. In addition to starting compound **1**, the most potent anti-schistosomal 3-phenoxymethyl

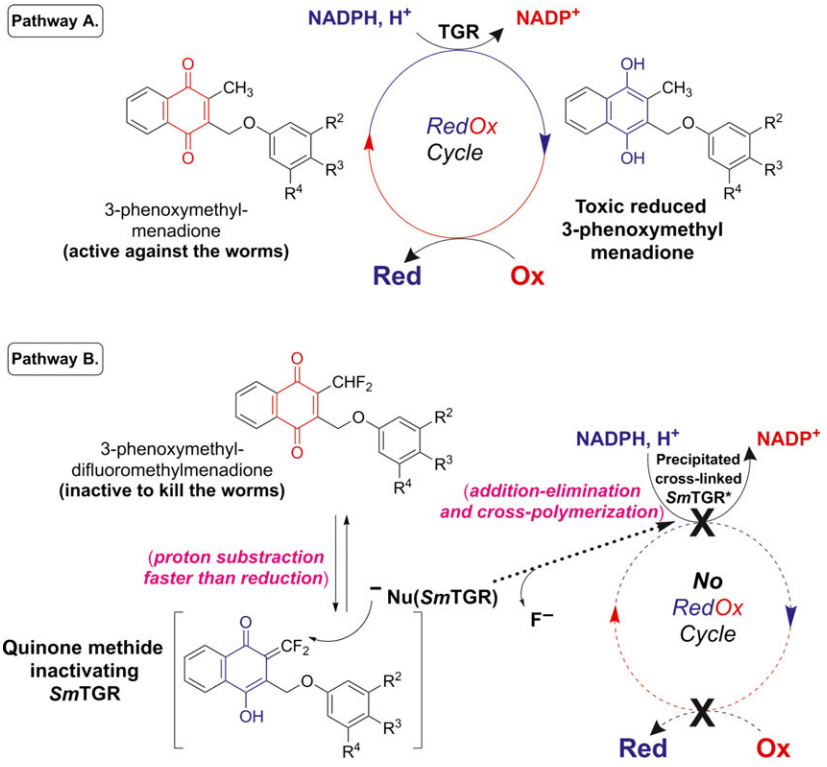

Fig. 5. Cascade of redox reactions responsible for the anti-schistosomal activity of 3-phenoxymethylmenadione derivatives such as compounds **2** or **7** (pathway A) and abolition of the toxicity by the suicide substrates, the difluoromethylmenadione analogs **8** or **9** (pathway B).

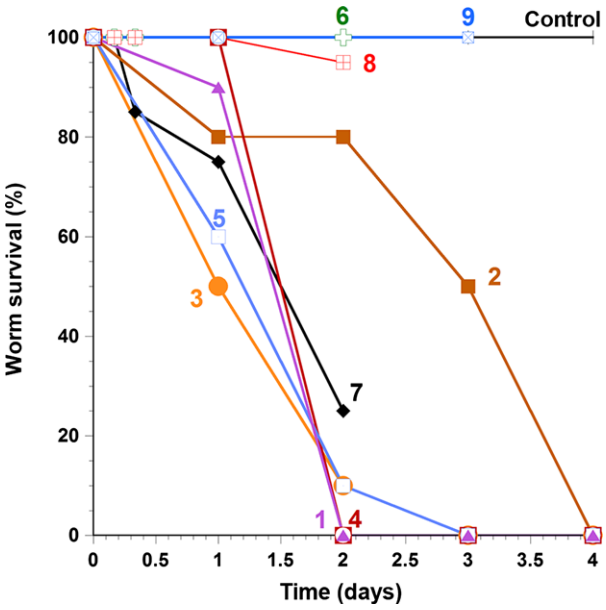

Fig. 6. Survival curves of *S. mansoni* worms cultured *in vitro* and treated with the representatives of 3-phenoxymethylmenadione series as indicated. Potassium antimonyl tartrate was used as a reference drug, killing 100% of the worms within 2 days (not shown).

menadiones were the compounds bearing the α–fluorophenol methyl ether in the oxyphenylmethylene arm, i.e. **3** and **7**, but not the difluoromethyl menadiones **8** and **9**. This may be explained based on the distinct mechanisms (Fig. 5). First, as predicted, the difluorophenol is known to mimic a carboxylic function [12], as in **1**, because the fluorine atoms are known to reduce the pK_a value of the phenol to lower values. The methyl ether of the phenol may increase the bioavailability in the worm and may release the phenol *in situ* in the worms [24]. Furthermore, due to the presence of several fluorine atoms, the compounds are thought to cross the lipophilic tegument of the worms effectively, in addition to conferring better metabolic stability *in vivo*. The bioisosteric effect of the difluorophenol (transiently protected as the methyl ether form) was validated using compound **7** (active) versus compound **6** (inactive), suggesting the importance of the pro-drug effect to release a 'negative' charge inside the parasite. In a second assay, all compounds were tested at 50 μM in the presence of hemoglobin (Hb) at 10 μM. After 7 h incubation with the lead compounds **1**-**5**, **7**, the majority of the worms were dead. After 22 h, all worms were dead whatever the compound tested. Interestingly, compound **2** showed a specific effect depending on the gender of the parasites, killing 100% of the female worms and only 50% of the male worms. These results suggest that compound **2** may affect a target that is particularly sensitive or more highly expressed in female worms than in male worms. The mechanism of action of **2** is still unclear, but it

may involve hemoglobin digestion, as female *Schistosoma* worms are known to have a higher hemoglobin intake and metabolism than males [25].

We also tested the activity of selected compounds against worms cultured *ex vivo* in the presence of human red blood cells (10 μL·well^{-1}). The purpose of adding human red blood cells is to allow worms to undergo drug bioactivation after hemoglobin digestion in the worm intestine. The final concentration of compounds was 50 μM. While survival rates 24 h after adding compound **7** were identical in the presence and absence of red blood cells, more parasites were dead in the absence of red blood cells than in the presence of red blood cells after 48 h. Their presence may increase the oxidative metabolism of compound **7**, and the reactive metabolites react quickly with electrophilic sites of non-essential components in the culture medium. Oxidative metabolism of **7** may lead to the generation of the phenol upon cleavage of the methoxy group or the phenoxymethyl bridge [23]. In this case, exposure to a Michael acceptor site (quinone methide) may be followed by thiol alkylation in the parasite [26].

Finally, as a proof of concept to validate the essential TGR-catalyzed bioactivation step for the observed anti-schistosomal activity of the 3-phenoxymethyl menadione series, the synthesis of a difluoromethyl analog (compound **8**, Fig. 1) of 3-phenoxymethyl menadione (compound **2**) was designed to alkylate *Sm*TGR *in situ* (i.e. in the parasite) by preventing formation of the corresponding reduced 3-phenoxymethyl menadione metabolite (dihydronaphthoquinone). This compound, 2-difluoromethyl-3-phenoxymethyl naphthoquinone (Fig. 1), was shown to act as a potent suicide substrate of isolated *Sm*TGR and *h*TrxR (Table 3). The introduction of two fluorines at the methyl group of menadione led to abolition of the anti-parasitic activity of the compound, i.e. compound **2** was (moderately) active whereas compound **8** was inactive. This result was confirmed using another pair of compounds: active compound **7** (without red blood cells) versus the inactive difluoromethyl analog, **9**. As shown in Fig. 6, neither compound **8** nor **9** showed any toxic effect on the worms, whether red blood cells were present or not. Hence, TGR inactivation by the bioreductible fluorinated alkylating (substituted phenoxy)methyl menadione derivatives *in situ* was directly correlated with abolition of the anti-schistosomal activity of the parent menadione analog **2**. Our data strongly support the requirement for an active TGR, within a cascade of redox reactions, to bioactivate potent anti-schistosomal 1,4-naphthoquinones. More studies are required to identify the cellular oxidant (Fig. 5) that is reduced in schistosomes, leading to death of the worms.

Cytotoxic activities against human cells *in vitro*

When tested for cytotoxicity against human lung MRC-5 fibroblasts, using the Alamar blue assay (Table S2), most of the 1,4-naphthoquinone derivatives were only mildly toxic (IC_{50} of 21.7–31.07 μM), with the exception of anti-schistosomal compound **1** (IC_{50} = 6.55 μM) and the difluoromethylmenadione derivatives **8** (IC_{50} = 6.70 μM) and **9** (IC_{50} = 11.20 μM). This cytotoxicity probably stems from the higher lipophilicity due to the presence of fluorine atoms and/or from their highly oxidant character [18].

In vivo anti-schistosomal activities of (substituted phenoxy)methyl menadiones in *S. mansoni*-infected mice

Selected compounds were tested in a laboratory model of *S. mansoni*. All injections were intraperitoneal, with the first being performed six weeks post-infection. Perfusions were performed 7 days after the last injection. The doses used were: **1**, four daily injections at 20 mg·kg^{-1} in 10% DMSO; **4**, 1 × 50 mg·kg^{-1} in 100% DMSO; **5**, four daily injections at 20 mg·kg^{-1} in 100% DMSO. Control animals received an equal volume of 10% DMSO. None of the compounds resulted in significant decreases in worm burdens. Furthermore, compound **1** was quite toxic, and three of five mice treated died. The remaining mice treated with compound **1** were severely affected.

Conclusions

We have designed and synthesized new 3-benzyloxo menadione and difluoromethylmenadione derivatives that show specific inhibitory activities *in vitro* against *Sm*TGR compared with *h*GR and *h*TrxR. Most of the compounds displayed sub-micromolar inhibitory activities toward *Sm*TGR. Structure–activity relationship studies showed high potential for (substituted phenoxy)methyl menadione derivatives to inhibit TGR in preference to GR or TrxR enzymes. Interestingly, one of these, the redox-active (4-methoxy-3-(trifluoromethyl) phenoxy) methyl menadione (**7**) showed time-dependent and NADPH-dependent SmTGR inactivation, correlating with potent anti-schistosomal action *in vitro*. The enzyme is expected to turn over in an unproductive redox cycle that ends in formation of an inactive TGR dimer as a reversible dead-end product. Therefore, redox-active 3-benzyloxo menadiones, such as **7**, may be considered inhibitors of possible half-site reactivity of *Sm*TGR because they may prevent transfer of the reactivity toward NADPH binding

of one subunit to the second subunit in order to allow disulfide reduction [21]. The formation of reversible dead-end flavoenzyme species as the reason for time- and NADPH-dependent *Sm*TGR inactivation by naphthoquinones is supported by the distinct time-dependent *Sm*TGR inactivation mechanism displayed by the difluoromethyl analog of inhibitor **7**, the difluoromethylmenadione derivative **9**. When *Sm*TGR was pre-incubated in the presence of the difluoromethylmenadione **9**, extremely rapid irreversible inactivation was found, and resulted in precipitation of a cross-linked and polymerized inactivated enzyme. However, the fact that the difluoromethylmenadione **9**, which inactivates *Sm*TGR through a non-consuming NADPH-dependent redox-active cycle, has little killing effect in worms cultured *ex vivo*, suggests that the effect of the other active compounds against *S. mansoni* worms, such as compound **7**, is due to continuous NADPH-consuming redox cycling of *Sm*TGR. Several analogs of compound **7** showed significant anti-schistosomal action against cultured parasites, but none of the compound tested were active in *S. mansoni-infected* mice *in vivo*. Limited bioavailability may compromise compound activity, and future studies will be directed toward improving this.

Experimental procedures

Chemistry

General methods and starting materials

Melting points were determined using a Büchi B-540 melting point apparatus (Büchi Labortechnik AG, Flawil, Switzerland). ^{1}H-NMR and ^{13}C-NMR spectra were recorded on Bruker ARX 250, Bruker DRX 300 or Bruker DRX 500 spectrometers (Bruker BioSpin GmBH, Rheinstetten, Germany) using $CDCl_3$, unless otherwise indicated. Chemical shifts (δ) are expressed in ppm relative to tetramethylsilane. Multiplicity is indicated as s (singlet), d (doublet), t (triplet), and m (multiplet). Har stands for an aromatic proton in ^{1}H-NMR. C^{IV} indicates a quaternary carbon in the ^{13}C-NMR signal assignment. *J* values are given in Hz. ^{19}F-NMR was performed using 1,2-difluorobenzene as external standard (δ = −139.0 ppm). Electron impact (EI) and fast atom bombardment (FAB) mass spectra (MS) were recorded at 70 eV on Jeol JMS-700 (Jeol Ltd., Tokyo, Japan) and Finnigan TSQ 700 (Thermo Fisher Scientific GmbH, Bremen, Germany) spectrometers at the Institut für Organische Chemie der Ruprecht-Karls Universität (Heidelberg, Germany). Elemental analyses (Anal.) were performed in the Mikroanalytisches Laboratorium der Chemischen Fakultät (Ruprecht-Karls Universität, Heidelberg, Germany). Analytical thin-layer chromatography (TLC) was performed on pre-coated Polygram® SIL G/UV_{254} silica gel plates. Silica gel G60 (230–400 mesh, Macherey-Nagel GmbH & Co. KG, Düren, Germany) was used for flash column chromatography. 1,4-dimethoxy-naphthalene, 1,4-dimethoxy-naphthalene-2-carbaldehyde, 2-(difluoromethyl)-1,4-dimethoxynaphthalene and 2-difluoromenadione were synthesized as previously described [17].

Side-chain elongation (general procedure 1)

The starting phenol (1.0 equivalents), ethylchloroacetate (1.15 equivalents), sodium iodide (1.0 equivalents), and anhydrous potassium carbonate (2.0 equivalents) were refluxed in dry acetone for 4 h. The mixture was cooled and filtered. The solid was washed with CH_2Cl_2 for 5 min at room temperature. The washing fraction was combined with the filtrate and evaporated *in vacuo*.

Kochi–Anderson reaction (general procedure 2)

Menadione (1.0 equivalents) and the starting phenoxyacetic acid (2.0 equivalents) were dissolved in a 3:1 solution of acetonitrile/H_2O, and heated to 85 °C. Silver nitrate (0.1 equivalents) was added first, and ammonium peroxodisulfate (1.3 equivalents) in solution in a 3 : 1 solution of acetonitrile/H_2O was added dropwise. The reaction mixture was stirred under reflux for 3 h. It was then cooled, and acetonitrile was removed *in vacuo*. The residue was extracted using CH_2Cl_2, dried over $MgSO_4$, and evaporated *in vacuo*. The crude mixture was purified by flash chromatography on silica gel and then recrystallization.

Synthesis of compounds

4-((3-methyl-1,4-dioxo-1,4-dihydronaphthalen-2-yl) methoxy)benzoic acid (compound 1)

Commercially available [4-(carboxy)phenoxy]acetic acid (2.27 g, 11.6 mmol) was used as the starting material and treated as described in general procedure 2. Recrystallization in pure acetone gave yellow crystals of the final derivative **1** (563 mg, 30%); melting point 222–223 °C; ^{1}H-NMR (300 MHz, [D6]DMSO): δ = 8.04–8.08 (m, 2H, Har), 7.87–7.94 (m, 4H, Har), 7.12 (d, 2H, Har), 5.16 (s, 2H), 2.23 (s, 3H); ^{13}C-NMR (75 MHz, [D6]DMSO): δ = 184.6 (C=O), 183.2 (C=O), 167.0, 161.7, 147.8 (C^{IV}), 138.8 (C^{IV}), 134.2, 131.5, 131.4, 126.0, 123.5, 121.3, 115.0, 61.0, 12.8; MS FAB *m/z*: 323.1 $[M+H]^+$; Anal. calcd for $C_{19}H_{14}O_5 \cdot 0.25\ H_2O$: C 69.83, H 4.47, found: C 69.94, H 4.55.

Ethyl 2-(4-cyanophenoxy)acetate (compound 2c)

Commercially available 4-cyanophenol (1 g, 8.40 mmol) was used as the starting material, and treated according to

general procedure 1. The crude product was obtained as a yellow oil. After flash chromatography purification using CH_2Cl_2, white crystals of **2c** were obtained (1.475 g, 86%); melting point 50–53 °C; ^{1}H-NMR (300 MHz, $CDCl_3$): δ = 7.58 (d, 2H, Har), 6.94 (d, 2H, Har), 4.66 (s, 2H), 4.26 (q, 2H), 1.28 (t, 3H); ^{13}C-NMR (75 MHz, $CDCl_3$): δ = 167.8, 160.9, 134.0, 118.8, 115.3, 105.0, 65.1, 61.6, 14.0; EI MS (70 eV, *m*/*z* (%)): 205.1 ($[M]^+$, 100), 132.1 (95), 102.1 (41); Anal. calcd for $C_{11}H_{11}NO_3$: C 64.38, H 5.40, N 6.83 found: C 64.37, H 5.44, N 6.79.

2-(4-cyanophenoxy)acetic acid (compound 2d)

Ethyl 2-(4-cyanophenoxy)acetate (compound **2c**, 500 mg, 2.44 mmol) was added to 50 mL of a 10% solution of KOH in MeOH, and the reaction mixture was refluxed for 5 h. The resulting solution was cooled and the solvent evaporated *in vacuo*. The residue was diluted with water and washed with Et_2O. The aqueous layer was then acidified and extracted using Et_2O. The organic layer was dried over $MgSO_4$ and concentrated *in vacuo* to give **2d** as a white solid (275 mg, 65%); melting point 169–172 °C; ^{1}H-NMR (300 MHz, [D6]DMSO): δ = 7.77 (d, 2H, Har), 7.09 (d, 2H, Har), 4.82 (s, 2H); ^{13}C-NMR (75 MHz, [D6] DMSO): δ = 169.5, 161.2, 134.1, 119.0, 115.6, 103.3, 64.6; EI MS (70 eV, *m*/*z* (%)): 177.07 ($[M]^+$, 86), 132.06 (100), 119.05 (34), 102.04 (63); Anal. calcd for $C_9H_7NO_3$: C 61.02, H 3.98, N 7.91, found: C 60.75, H 4.01, N 7.76.

4-((3-methyl-1,4-dioxo-1,4-dihydronaphthalen-2-yl) methoxy)benzonitrile (compound 2)

Compound **2d** (200 mg, 1.12 mmol) was used as the starting material and treated according to general procedure 2. Flash chromatography purification using hexane/EtOAc (4:1) gave final derivative **2** as a yellow solid (40 mg, 24%); melting point 181–183 °C; ^{1}H-NMR (300 MHz, $CDCl_3$): δ = 8.10–8.55 (m, 2H, Har), 7.72–7.76 (m, 2H, Har), 7.39 (d, 2H, Har), 6.87 (d, 2H, Har), 5.10 (s, 2H), 2.31 (s, 3H); ^{13}C-NMR (75 MHz, $CDCl_3$): δ = 184.9 (C=O), 183.5 (C=O), 161.6, 148.7 (C^{IV}), 138.9 (C^{IV}), 134.1, 134.0, 132.1, 131.7, 126.6, 119.0, 115.4, 104.8, 61.0, 13.3; EI MS (70 eV, *m*/*z* (%)): 303.1 ($[M]^+$, 100), 185.1 (94), 157.1 (96), 128.1 (40); Anal. calcd for $C_{19}H_{13}NO_3$: C 75.24, H 4.32, N 4.62, found: C 75.40, H 4.22, N 4.51.

2,6-difluorobenzene-1,4-diol (compound 3a)

The 2,6-difluorophenol (200 mg, 1.54 mmol) was dissolved in 10 mL of 6% NaOH. Solid potassium persulfate (425 mg, 1.55 mmol) was added to this stirred solution in several portions over 10 min. The orange mixture was stirred overnight at room temperature. It was then concentrated to a third of its original volume on a rotary evaporator. The solution was neutralized using concentrated HCl and extracted using water. The aqueous solution was acidified using 3 mL concentrated HCl, and boiled for 1 h. It was then concentrated to a quarter of its original volume on the rotary evaporator. Addition of 10 mL acetone precipitated the inorganic salts, which were removed via filtration. The filtrate was evaporated *in vacuo*. The brown residue was dissolved in acetone and added to silica gel. The solvent was removed, and the material was added to a column of silica gel. Flash chromatography purification using hexane/EtOAc (2:1) gave compound **3a** as a white solid (100 mg, 44%); melting point 149–151 °C; ^{1}H-NMR (300 MHz, [D_6]DMSO): δ = 9.55 (s, 1H, Ph-O<u>H</u>), 9.14 (s, 1H, Ph-O<u>H</u>), 6.36–6.43 (m, 2H, Har); ^{13}C (75 MHz, [D_6]DMSO): δ = 152.8 (dd, $^1J_{C\text{-}F}$ = 239.9 Hz, $^3J_{C\text{-}F}$ = 9.4 Hz, 2C), 149.6 (t, $^3J_{C\text{-}F}$ = 13.2 Hz), 125.7 (t, $^2J_{C\text{-}F}$ = 16.7 Hz), 99.2 (dd, $^2J_{C\text{-}F}$ = 25.1 Hz, 2C); EI MS (70 eV, *m*/*z* (%)): 146.06 ($[M]^+$, 100), 98.04 (18), 70.03 (23); Anal. calcd for $C_6H_4F_2O_2$: C 49.33, H 2.76, found: C 49.08, H 2.87.

Ethyl 2-(3,5-difluoro-4-methoxyphenoxy)acetate (compound 3c)

3,5-difluoro-4-methoxyphenol (compound **3b**, 500 mg, 3.12 mmol) was used as the starting material and treated according to general procedure 1. The crude product was obtained as a yellow oil. Flash chromatography purification using CH_2Cl_2 led to white crystals of **3c** (720 mg, 94%); melting point 29–30 °C; ^{1}H-NMR (300 MHz, $CDCl_3$): δ = 6.40–6.51 (m, 2H, Har), 4.52 (s, 2H), 4.24 (q, 2H), 3.87 (s, 3H), 1.27 (t, 3H); ^{13}C-NMR (75 MHz, $CDCl_3$): δ = 168.1, 156.2 (dd, $^1J_{C\text{-}F}$ = 247.5 Hz, $^3J_{C\text{-}F}$ = 8.1 Hz, 2C), 153.1 (t, $^3J_{C\text{-}F}$ = 12.8 Hz), 131.2 (t, $^2J_{C\text{-}F}$ = 14.8 Hz), 99.4 (dd, $^2J_{C\text{-}F}$ = 26.6 Hz, 2C), 65.7, 62.0 (t, $^4J_{C\text{-}F}$ = 2.8 Hz), 61.5, 14.0; EI MS (70 eV, *m*/*z* (%)): 246.1 ($[M]^+$, 100), 173.08 (26), 159.06 (34), 145.05 (14); Anal. calcd for $C_{11}H_{12}F_2O_4$: C 53.66, H 4.91, found: C 53.51, H 4.88.

2-(3,5-diffluoro-4-methoxyphenoxy)acetic acid (compound 3d)

The ethyl ester **3c** (500 mg, 2.03 mmol) was hydrolysed in 25 mL of 10% aqueous NaOH. After refluxing the mixture for 2 h, it was cooled and then acidified with concentrated HCl, whereupon the acid crystallized as a white solid. The suspension was filtered and the precipitate dried to obtain **3d** as a white solid (340 mg, 77%); melting point 115–117 °C; ^{1}H-NMR (300 MHz, [D6]DMSO): δ = 6.80 (d, 2H, Har), 4.68 (s, 2H), 3.82 (s, 3H); ^{13}C-NMR (75 MHz, [D6] DMSO): δ = 169.7, 155.6 (dd, $^1J_{C\text{-}F}$ = 244.8 Hz, $^3J_{C\text{-}F}$ = 8.4 Hz, 2C), 153.5 (t, $^3J_{C\text{-}F}$ = 13.3 Hz), 129.9 (t, $^2J_{C\text{-}F}$ = 15.1 Hz), 99.6 (dd, $^2J_{C\text{-}F}$ = 26.1 Hz, 2C), 65.2, 62.1 (t, $^4J_{C\text{-}F}$ = 2.4 Hz); EI MS (70 eV, *m*/*z* (%)): 218.09 ($[M]^+$, 100), 203.06 (19), 159.06 (54), 145.04 (60), 125.03 (26); Anal.

calcd for $C_9H_8F_2O_4$: C 49.55, H 3.70, found: C 49.29, H 3.67.

2-((3,5-difluoro-4-methoxyphenoxy)methyl)-3-methylnaphthalene-1,4-dione (compound 3)

Compound **3d** was used as the starting material and treated according to general procedure 2. Flash chromatography purification using hexane/EtOAc (10:1) gave the final derivative **3** as a light yellow powder (55 mg, 41%); melting point 181–183 °C; ^{1}H-NMR (300 MHz, $CDCl_3$): δ = 8.13 (m, 2H, Har), 7.75 (m, 2H, Har), 8.56 (d, 2H, Har), 5.04 (s, 2H), 3.91 (s, 3H), 2.31 (s, 3H), ^{13}C-NMR (75 MHz, $CDCl_3$): δ = 185.0 (C=O), 183.5 (C=O), 156,3 (dd, $^1J_{C\text{-}F}$ = 247.4 Hz, $^3J_{C\text{-}F}$ = 8.2 Hz, 2C), 153.8 (t, $^3J_{C\text{-}F}$ = 12.7 Hz), 148.5 (C^{IV}), 139.1 (C^{IV}), 133.9, 132.1, 131.7, 131.1 (t, $^2J_{C\text{-}F}$ = 14.8 Hz), 126.6, 99.4 (dd, $^2J_{C\text{-}F}$ = 26.4 Hz, 2C), 62.2 (t, $^4J_{C\text{-}F}$ = 2.7 Hz), 61.4, 13.2; EI MS (70 eV, *m*/*z* (%)): 344.1 ($[M]^+$, 61), 160.1 (100); Anal. calcd for $C_{19}H_{14}F_2O_4$: C 66.28, H 4.10, found: C 65.87, H 4.31.

2-((4-chlorophenoxy)methyl)-3-methylnaphthalene-1,4-dione (compound 4)

Commercially available [4-(chloro)-phenoxy]acetic acid (2.16 g, 11.6 mmol) was used as the starting material and treated according to general procedure 2. Flash chromatography purification using petroleum ether/Et_2O (4:1) gave compound **4** (633 mg, 35%); melting point 106–108 °C; ^{1}H-NMR (300 MHz, $CDCl_3$): δ = 8.10–8.15 (m, 2H, Har), 7.73–7.76 (m, 2H, Har), 7.25 (d, 2H, Har), 6.92 (d, 2H, Har), 5.10 (s, 2H), 2.32 (s, 3H); ^{13}C-NMR (75 MHz, $CDCl_3$): δ = 185.1 (C=O), 183.6 (C=O), 157.0, 148.4 (C^{IV}), 139.6 (C^{IV}), 133.8, 132.0, 131.8, 129.4, 126.5, 126.3, 116.1, 61.1, 13.2; MS FAB *m*/*z*: 313.1 $[M+H]^+$; Anal. calcd for $C_{18}H_{13}ClO_3$: C 69.13, H 4.19, Cl 11.34 found: C 69.35, H 4.20.

2-((4-bromophenoxy)methyl)-3-methylnaphthalene-1,4-dione (compound 5)

Commercially available [4-(bromo)-phenoxy]acetic acid (2.68 g, 11.6 mmol) was used as the starting material and treated according to general procedure 2. Flash chromatography purification using petroleum ether/Et_2O (4:1) gave the final derivative **5** (500 mg, 24%); melting point 108–110 °C; ^{1}H-NMR (300 MHz, $CDCl_3$): δ = 8.10–8.15 (m, 2H, Har), 7.73–7.76 (m, 2H, Har), 7.39 (d, 2H, Har), 6.87 (d, 2H, Har), 5.10 (s, 2H), 2.32 (s, 3H); ^{13}C-NMR (75 MHz, $CDCl_3$): δ = 185.1 (C=O), 183.6 (C=O), 157.5, 148.4 (C^{IV}), 139.6 (C^{IV}), 133.8, 132.4, 126.5, 116.6, 113.7, 61.0, 13.2; MS FAB *m*/*z*: 357.1 $[M+H]^+$; Anal. calcd for $C_{18}H_{13}BrO_3$: C 60.52, H 3.67, found: C 60.73, H 3.82.

2-methyl-3-((3-(trifluoromethyl)phenoxy) methyl)naphthalene-1,4-dione (compound 6)

Commercially available [3-(trifluoromethyl)phenoxy]acetic acid (500 mg, 2.28 mmol) was used as the starting material and treated according to general procedure 2. Flash chromatography purification using hexane/EtOAc (10:1) gave yellow crystals of the final derivative **6** (80 mg, 20%); melting point 106–108 °C; ^{1}H-NMR (300 MHz, $CDCl_3$): δ = 8.14 (m, 2H, Har), 7.75 (m, 2H, Har), 7.41 (m, 1H, Har), 7.14–7.26 (m, 3H, Har), 5.16 (s, 2H), 2.34 (s, 3H); ^{13}C-NMR (75 MHz, $CDCl_3$): δ = 184.0 (C=O), 181.5 (C=O), 139.4, 133.9, 133.8, 130.1, 126.6, 126.5, 118.1, 112.1 (q, $^3J_{C\text{-}F}$ = 3.9 Hz), 111.7, 111.6, 61.0, 13.2; ^{19}F-NMR (282 MHz, $CDCl_3$): δ = - 63.10; EI MS (70 eV, *m*/*z* (%)): 346.1 ($[M]^+$, 100), 331.1 (21), 201.1 (21), 185.1 (61), 157.1 (83), 128.1 (39); Anal. calcd for $C_{19}H_{13}F_3O_3$: C 65.90, H 3.78, found: C 65.87, H 4.03.

Ethyl 2-(4-methoxy-3-(trifluoromethyl)phenoxy)acetate (compound 7c)

Commercially available 4-methoxy-3-trifluoromethyl phenol (550 mg, 2.86 mmol) was used as the starting material and treated according to general procedure 1. The pure product **7c** was obtained as a white solid (760 mg, 2.73 mmol, 95%); melting point 63–64 °C; ^{1}H-NMR (300 MHz, $CDCl_3$): δ = 7.16 (d, 1H, Har), 7.05 (dd, 1H, Har), 6.93 (d, 1H, Har), 4.59 (s, 2H), 4.27 (q, 2H), 3.86 (s, 3H), 1.30 (t, 3H); ^{13}C-NMR (75 MHz, $CDCl_3$): δ = 168.7 (C=O), 152.4 (C^{IV}), 151.2 (C^{IV}), 123.2 (q, $^1J_{C\text{-}F}$ = 272.5 Hz, CF_3), 119.5 (q, $^2J_{C\text{-}F}$ = 31.2 Hz), 118.9, 114.3, 113.4, 66.3, 61.5, 56.5, 14.1; ^{19}F-NMR (282 MHz, $CDCl_3$): δ = - 62.97; EI MS (70 eV, *m*/*z* (%)): 278.1 ($[M]^+$, 100), 205.08 (33), 191.05 (54); Anal. calcd for $C_{12}H_{13}F_3O_4$: C 51.80, H 4.71; found: C 51.48, H 4.66.

2-(4-methoxy-3-(trifluoromethyl)phenoxy)acetic acid (compound 7d)

The ethyl ester (500 mg, 1.80 mmol) was hydrolysed in 25 mL of 10% aqueous NaOH. After refluxing the mixture for 2 h, it was cooled and then acidified using concentrated HCl, whereupon the acid crystallized as a white solid. The suspension was filtered and the precipitate dried to obtain **7d** as a white solid (415 mg, 92%); melting point 133–135 °C; ^{1}H-NMR (300 MHz, [D_6]DMSO): δ = 7.20 (m, 2H, Har), 7.13 (m, 1H, Har), 4.71 (s, 2H), 3.82 (s, 3H); ^{13}C-NMR (75 MHz, [d6]DMSO): δ = 170.1 (C=O), 151.3 (C^{IV}), 151.0 (C^{IV}), 119.7, 114.2, 113.1, 65.2, 56.4; ^{19}F-NMR (282 MHz, [D_6]DMSO): δ = - 61.17; EI MS (70 eV, *m*/*z* (%)): 250.1 ($[M]^+$, 90), 191.1 (94), 177.0 (21), 129.0 (19); Anal. calcd for $C_{10}H_9F_3O_4$: C 48.01, H 3.63; found: C 47.75, H 3.62.

2-((4-methoxy-3-(trifluoromethyl)phenoxy)methyl)-3-methylnaphthalene-1,4-dione (compound 7)

2-(4-methoxy-3-(trifluoromethyl)phenoxy)acetic acid (compound **7d**, 400 mg, 1.60 mmol) was used as the starting material and treated according to general procedure 2. Flash chromatography purification using hexane/EtOAc (10:1) gave the final derivative **7** as yellow crystals (59 mg, 20%); melting point 146–148 °C; ^{1}H-NMR (300 MHz, $CDCl_3$): δ = 8.10–8.15 (m, 2H, Har), 7.72–7.76 (m, 2H, Har), 7.22 (d, 1H, Har), 7.12 (dd, 2H, Har), 6.95 (d, 1H, Har), 5.09 (s, 2H), 3.86 (s, 3H), 2.32 (s, 3H); ^{13}C-NMR (75 MHz, $CDCl_3$): δ = 185.2 (C=O), 183.6 (C=O), 152.1 (C^{IV}), 151.7 (C^{IV}), 148.3 (C^{IV}), 139.6 (C^{IV}), 133.8, 132.1 (C^{IV}), 131.8 (C^{IV}), 126.6, 123.3 (q, $^{1}J_{C\text{-}F}$ = 272.7 Hz, CF_3), 119.5 (q, $^{2}J_{C\text{-}F}$ = 31.2 Hz), 118.9, 114.2 (q, $^{3}J_{C\text{-}F}$ = 5.4 Hz), 113.5, 61.7, 56.6, 13.2; ^{19}F-NMR (282 MHz, $CDCl_3$): δ = - 63,09; EI MS (70 eV, *m*/*z* (%)): 376.2 ($[M]^+$, 66), 192.1 (100), 191.1 (80), 157.1 (25), 128.1 (19), 127.1 (7), Anal. calcd for $C_{20}H_{15}F_3O_4$: C 63.83, H 4.02, found: C 63.56, H 4.19.

4-((3-(difluoromethyl)-1,4-dioxo-1,4-dihydronaphthalen-2-yl)methoxy)benzonitrile (compound 8)

Compound **2d** (1 g, 5.64 mmol) and difluoromenadione (600 mg, 2.8 mmol) were used as the starting materials and treated according to general procedure 2. Flash chromatography purification using hexane/EtOAc (2:1) gave the final derivative **8** as a yellow solid (344 mg, 35%); melting point 143–145 °C; ^{1}H-NMR (300 MHz, $CDCl_3$): δ = 8,17 (m, 2H, Har); 7,84 (m, 2H, Har); 7,62 (d, 2H, Har); 7,17 (t, $^{2}J_{H\text{-}F}$ = 53,5 Hz, CHF_2); 7,04 (d, 2H, Har); 5,29 (s, 2H);^{13}C-NMR (75 MHz, $CDCl_3$): δ = 175.9 (C=O), 174.5 (C=O); 161.5 (C^{IV}), 142.5 (C^{IV}), 138.2 (t, $^{2}J_{C\text{-}F}$ = 21 Hz), 134.9, 134.8, 134.10 (2C), 131.5 (C^{IV}), 131.1 (C^{IV}), 127.1, 126.8, 119.0 (C^{IV}), 115.5 (2C), 110.1(t, $^{1}J_{C\text{-}F}$ = 241 Hz), 105.0 (C^{IV}), 60.0; ^{19}F-NMR (282 MHz, $CDCl_3$): δ = −116.36; EI MS (70 eV, *m*/*z* (%)): 340.3 ($[M]^+$, 100), Anal. calcd for $C_{19}H_{11}F_2NO_3{\cdot}0.5\ H_2O$: C 67.26, H 3.27, N 4.13; found: C 67.33, H 3.43, N 4.12.

2-(difluoromethyl)-3-((4-methoxy-3-(trifluoromethyl) phenoxy)methyl)naphthalene-1,4-dione (compound 9)

2-(4-methoxy-3-(trifluoromethyl)phenoxy)acetic acid (compound **7d,** 2.40 g, 9.6 mmol) and difluoromenadione (1 g, 4.8 mmol) were used as the starting materials and treated according to general procedure 2. Flash chromatography purification using hexane/EtOAc (10:1) gave **9** as an orange solid (1.116 g, 2.71 mmol, 57%); melting point 84–86 °C; ^{1}H-NMR (300 MHz, $CDCl_3$): δ = 8.15–8.18 (m, 2H, Har), 7.82–7.85 (m, 2H, Har), 7.23 (d, $^{4}J_{H\text{-}H}$ = 3 Hz, 1H, Har), 7.17 (t, $^{2}J_{H\text{-}F}$ = 54 Hz, 1H, CHF_2), 7.14 (dd, $^{3}J_{H\text{-}H}$ = 9 Hz, $^{4}J_{H\text{-}H}$ = 3 Hz, 1H, Har), 6.96 (d, $^{3}J_{H\text{-}H}$ = 9 Hz, 1H, Har), 5.21 (s, 2H), 3.87 (s, 3H); ^{13}C-NMR (75 MHz, $CDCl_3$): δ = 183.4 (C=O), 182.6 (C=O), 152.4 (C^{IV}), 151.7 (C^{IV}), 143.3 (C^{IV}), 137.8 (t, $^{2}J_{C\text{-}F}$ = 21 Hz), 134.8, 134.7, 131.6 (C^{IV}), 131.2 (C^{IV}), 127.1, 126.8, 126.2 (q, $^{1}J_{C\text{-}F}$ = 272.5 Hz, CF_3), 119.5, 119.4 (q, $^{2}J_{C\text{-}F}$ = 31.2 Hz), 114.7 (q, $^{3}J_{C\text{-}F}$ = 5 Hz), 113.5, 110.2 (t, $^{1}J_{C\text{-}F}$ = 241 Hz), 61.1, 56.6; ^{19}F-NMR (282 MHz, $CDCl_3$): δ = −116.98 (d, $J_{H\text{-}F}$ = 54 Hz, CHF_2), δ = −62.48 (CF_3); −116.98; MS FAB *m*/*z*: 412.3 ($[M]^+$); Anal. calcd for $C_{20}H_{13}F_5O_4$: C 58.26, H 3.18, found: C 57.96, H 3.35.

Cyclic voltammetry

Cyclic voltammetry of the menadione derivatives (approximately 10^{-3} M) was performed using a Voltalab 50 potentiostat/galvanostat (Radiometer Analytical MDE15 polarographic stand, PST050 analytical voltammetry and CTV101 speed control unit, Radiometer Analytical, CTB Choffel dealer, Remiremont, France) controlled by Voltamaster 4 electrochemical software. A conventional three-electrode cell (10 mL) was used in our experiments, comprising a glassy carbon disk (GC, s = 0.07 cm^2) set into a Teflon rotating tube as a working electrode, a Pt wire as a counter electrode, and a KCl (3 M)/Ag/AgCl reference electrode (+210 mV versus normal hydrogen electrode) [27]. Prior to each measurement, the surface of the GC electrode was carefully polished with 0.3 μm aluminium oxide suspension (Escil, Chassieux, France) on a silicon carbide abrasive sheet (grit 800/2400). Thereafter, the GC electrode was thoroughly washed with water, and dried with paper towels and argon. In all experiments, used water was distilled and further purified by passing it through a mixed bed of ion-exchanger (Bioblock Scientific R3-83002, M3-83006, Illkirch, France) and activated carbon (Bioblock Scientific ORC-83005, Illkirch, France) and was de-oxygenated with CO_2- and O_2-free argon (Oxiclear cartridge, Sigma-Aldrich, Saint Quentin Fallavier, France) before use. The electrode was installed into the voltammetry cell together with a platinum wire counter electrode and the reference (Ag/AgCl 3M KCl). Solutions containing menadione derivatives (approximately 10^{-3} M) were vigorously stirred and purged using O_2-free argon for 15 min before the voltammetry experiment was initiated and maintained under an argon atmosphere during the measurement procedure. The voltammograms were recorded at room temperature (23 °C) in DMSO with 100 mM tetra-*n*-butylammonium hexafluorophosphate as the inert electrolyte. The voltage sweep rate was varied from 50 to 300 $mV{\cdot}s^{-1}$, and cyclic voltammograms were recorded from +0.5 to −2.2 V. Peak potentials were measured at a scan rate of 200 $mV{\cdot}s^{-1}$. Redox potentials were determined from oxidation and reduction potentials.

Glutathionylation reactions

GSH conjugates were prepared by incubating difluoromethylmenadione or its derivatives **8** and **9** with five

equivalents of reduced glutathione. Reduced glutathione was purchased from Sigma-Aldrich, and a fresh stock solution (100 mM) was prepared daily by dissolving in purified distillated water. Stock solutions (10 mM) of difluoromethylmenadione and its derivatives **8** and **9** were prepared in acetonitrile and kept at 4 °C. Glutathionylation of the difluoromethylmenadione and its derivatives **8** and **9** was first investigated by LC-MS and UV-Vis spectrophotometry over a 1 h period at 25 °C. All reaction mixtures (final volume 500 μL) used in the UV-Vis and LC-MS analyses contained 200 μL acetonitrile, 1 mM GSH (25 μL of a 20 mM stock solution in pure water), 200 μM naphthoquinone (10 μL of the 10 mM stock solution in acetonitrile) and 265 μL of an aqueous solution adjusted to pH 7.5 with aqueous NH_4OH. For the LC-MS analysis, 10 μL formic acid (50% solution) was used to stop the GSH reaction. In contrast, UV-Vis spectra were recorded as soon as the buffer was added. In parallel, an additional control without acetonitrile was prepared for compound **8** in an aqueous buffer adjusted to pH 7.5 with aqueous NH_4OH. Slight modifications of the protocols for the glutathionylation reactions were used for the LC-MS analyses, in particular in order to optimize the m/z signals by increasing the starting naphthoquinone and GSH concentrations fivefold. All reaction mixtures (final volume of 500 μL) used in the LC-MS analysis contained 160 μL acetonitrile, 5 mM GSH (25 μL of the 100 mM stock solution), 1 mM naphthoquinone (50 μL of the 10 mM stock solution), 265 μL of an aqueous buffer adjusted at pH 7.5 with aqueous NH_4OH, and 10 μL of 50% formic acid solution. At various time points (0, 1, 2, 4 and 24 h), 5 μL aliquots of each reaction mixture were removed and analyzed by LC-MS and UV-Vis spectrophotometry for GSH conjugate formation (see Methods S1 for details of the LC–MS analyses).

Enzymes

Recombinant human glutathione reductase was purified as described previously [28], and had a specific activity of 182 $U \cdot mg^{-1}$ (9500 units·μmol^{-1} subunit). Recombinant *Sm*TGR was expressed in *Escherichia coli* and purified by affinity chromatography as described previously [11].

*Sm*TGR inhibitory activity

Reduction of DTNB by *Sm*TGR was used to determine the potencies of all compounds. *Sm*TGR was pre-incubated with 100 μM NADPH and 50 μM compounds at room temperature for 10 min in reaction buffer (100 mM potassium phosphate, pH 7.4, 10 mM EDTA). Then, 3 mM DNTB and 100 μM NADPH were added to initiate the reactions. The rate of formation of 2-nitro-5-thiobenzoic acid from DTNB was determined spectrally using an $\varepsilon_{412\ nm}$ of 13.6 $mM^{-1} \cdot cm^{-1}$. The absorbance of each reaction was followed using a Multiskan Spectrum microplate spectrophotometer (ThermoFisher Scientific OY, Vantaa, Finland) with an experimentally determined pathlength correction factor. To determine the IC_{50} values against TGR in enzymic assays, compounds were tested at multiple concentrations between 0.01 and 30 mM. The DTNB reduction by *S. mansoni* TGR treated with various compounds was compared to that of untreated enzyme pre-incubated with 100 μM NADPH but without inhibitor.

Time-dependent inactivation of SmTGR by compound 7 or compound 9

To determine the rate constants of *S. mansoni* TGR inactivation by compound **7** (Fig. 4A,B), the residual DTNB reduction activity was monitored over time by following an incubation protocol [29]. Stock solutions (10 mM) of compound **7** and compound **9** were prepared in DMSO and kept at 25 °C. All pre-reaction mixtures (final volume of 100 μL) contained 100 μM NADPH, varying inhibitor concentrations (0–10 μM), *Sm*TGR (40 nM) and 1.8% DMSO in TGR buffer at 25 °C. At various time points (0, 2.5, 5.0 and 10.0 min), 100 μL of reaction buffer (3 mM DTNB and 100 μM NADPH in TGR buffer) was added to each pre-reaction, and residual activity was measured by the standard DTNB reduction assay at 25 °C. In the case of inhibitor **9**, SmTGR inactivation at various inhibitor concentrations (0–10 μM) was tested with pre-incubation times of 0 and 5 min, with and without NADPH in TGR buffer at 25 °C (Fig. 4C). The final DMSO concentration in all assays was 3.4%.

*h*GR inhibitory activity

The standard assay for *h*GR inhibitory activity was performed at 25 °C as described previously [17]. Briefly *h*GR was added to the assay mixture, which contained 100 μM NADPH, 1 mM glutathione disulfide, and the inhibitor (0–100 μM) in buffer (100 mM potassium phosphate buffer, 200 mM KCl, 1 mM EDTA, pH 6.9). The reaction was started by adding *h*GR, and initial rates of NADPH oxidation were monitored at 340 nm ($\varepsilon_{340\ nm}$ = 6.22 $mM^{-1} \cdot cm^{-1}$), and IC_{50} was calculated.

*h*TrxR inhibitory activity

Wild-type human placental *h*TrxR, the recombinant *h*TrxR mutant Sec498C and *h*TrxC72S were purified/recombinantly produced and assayed on a Hitachi U-2100 spectrophotometer (Hitachi, Krefeld, Germany) as previously described [30]. Inhibition studies on the wild-type enzyme were performed using the thioredoxin assay as well as the DTNB assay. Due to a loss of thioredoxin-reducing activity, the Sec498C mutant was assayed using the DTNB assay only. Half-maximal inhibition of the enzymes was determined by incubating wild-type *h*TrxR (5–25 nM

FAD-containing subunits) or mutant *h*TrxR (2 μM FAD-containing subunits) for 10 min with NADPH (100 or 200 μM) and inhibitor at 25 °C. The enzyme activity was then measured at 340 or 412 nm by adding *h*TrxC72S (20 μM) or DTNB (3 mM) to the mixtures.

Evaluation of the cytotoxicity of the various compounds against human MRC-5 cells

Human MRC-5_{SV2} cells were cultured in Earl's modified Eagle's medium + 5% fetal bovine serum. Assays were performed in 96-well microtiter plates, each well containing approximately 10^4 cells. After 3 days of incubation, cell viability was assessed fluorimetrically after adding resazurin, and fluorescence was measured at λ_{ex} 550 nm, λ_{em} 590 nm [31]. The results are expressed as the percentage reduction in cell growth/viability compared to untreated control wells, and IC_{50} was determined. Compounds were tested at five concentrations (64, 14, 4, 1 and 0.25 μM). When the IC_{50} is lower than 4 μM, the compound is classified as toxic.

Anti-schistosomal activity against adult worms cultured *ex vivo*

Adult worms were harvested by perfusing mice with Dulbecco's modified Eagle's medium 6–7 weeks after infection with *S. mansoni* [32]. Harvested worms were washed thoroughly with Dulbecco's modified Eagle's medium. The parasites were then cultured in RPMI 1640 medium containing 2 mM glutamine, 25 mM HEPES, 10% heat-inactivated fetal bovine serum, 125 $\mu g \cdot mL^{-1}$ streptomycin and 150 $units \cdot mL^{-1}$ penicillin G in a CO_2 incubator at 37 °C overnight. Overnight culture allows the worms to recover from the nembutal anesthesia used to euthanize the mice and adapt to the culture medium. All compounds were dissolved in DMSO, and their activities were tested against adult worms at a concentration of 50 μM. The mobility of the parasites was observed under a stereomicroscope over a 48 h period. The parasites were considered dead after they had completely lost mobility. Human red blood cells were isolated by centrifuging whole blood at 400 ***g*** without breaks for 10 min. The pelleted cells were washed three times with RPMI + 10% fetal bovine serum. Finally, the wash supernatant was removed, and the cells were resuspended in the same volume of RPMI + 10% fetal bovine serum as the initial blood sample. Worms were cultured in the presence of 10 μL human red blood cells per well. When present in the cultures, hemoglobin (human, Sigma-Aldrich) was used at 10 μM.

In vivo drug treatments

Compounds were dissolved in DMSO and administered by intraperitoneal injection as indicated above. Control *S. mansoni*-infected mice were injected with a corresponding amount of DMSO. Worm burdens were determined via hepatoportal perfusion 7 days after the last drug administration.

Animal welfare

This study was approved by the Institutional Animal Care and Use Committee at Rush University Medical Center (IACUC number 11-064; DHHS animal welfare assurance number A3120-01). Rush University Medical Center's Comparative Research Center (CRC) is operated in accordance with the Animal Welfare Act [Public Law (P.L.) 89-544, as amended by P.L.91-579 (1970), P.L.94-279 (1976), P.L. 99-198(1985) and P.L 101-624 (1990)], the Public Health Service's Policy on Humane Care and Use of Laboratory Animals (revised 2002), the Guide for the Care and Use of Laboratory Animals (revised 1996) and the US Government Principles for the Utilization and Care of Vertebrate Animals Used in Testing, Research and Training. The CRC is registered with the Animal and Plant Health Inspection Service of the US Department of Agriculture. The Institution has an Animal Welfare Assurance on file with the National Institutes of Health, Office of Laboratory Animal Welfare (A-3120-01). The facilities are accredited by the Association for Assessment and Accreditation of Laboratory Animal Care International. The CRC is directed by the Senior Director of the CRC, who is a doctor of veterinary medicine, holds a diploma from the American College of Laboratory Animal Medicine, and reports to the Associate Provost and Vice President for Research, who is also the Institutional Official for Animal Care and Use.

Acknowledgements

The authors thank Mourad Elhabiri and Mouhamad Jida for assistance with interpretation of the results of the electro- and physico-chemistry and mass spectrometry analysis of the GSH conjugates. E. D.-C. is grateful to Prof. Louis Maes, Antwerp University, for drug cytotoxicity measurements with the human cell line MRC-5. This work was partly supported by the ANRémergence Program (grant SCHISMAL to E. D-C.), the Laboratoire d'Excellence (LabEx) ParaFrap (grant LabEx ParaFrap ANR-11-LABX-0024 to E. D.-C.), the National Institutes of Health/National Institute of Allergy and Infectious Disease (grant R01AI065622 to D.L.W.), and the Deutsche Forschungsgemeinschaft (BE1540/11-2 to K.B.). Schistosome-infected mice were provided by the National Institute of Allergy and Infectious Disease Schistosomiasis Resource Center at the Biomedical Research Institute (Rockville, MD) through National Institutes of Health/National Institute of Allergy and Infectious

Disease contract HHSN272201000005I distributed through BEI Resources (Manassas, VA).

Author contributions

E.D.-C. conceived the medicinal chemistry approach, and L.J. contributed to synthesis of the naphthoquinones. E.D.-C. and D.B. co-wrote the manuscript. L.J. and H.-H.H. implemented the chemistry and parasitology protocols, respectively. D.B. and M.C. performed electrochemical, UV-Vis spectrophotometry, and LC-MS measurements. K.B. and D.L.W. supervised the enzymic studies and wrote the corresponding parts of the manuscript. D.L.W. analyzed the parasitological data and revised the manuscript. All authors produced the figures and commented on the manuscript.

References

1 Jordan P (2000) From katayama to the Dakhla oasis: the beginning of epidemiology and control of bilharzia. *Acta Trop* **77**, 9–40.
2 Gryseels B, Polman K, Clerinx J & Kestens L (2006) Human schistosomiasis. *Lancet* **368**, 1106–1118.
3 Steinmann P, Keiser J, Bos R, Tanner M & Utzinger J (2006) Schistosomiasis and water resources development: systematic review, meta-analysis, and estimates of people at risk. *Lancet Infect Dis* **6**, 411–425.
4 Chitsulo L, Engels D, Montresor A & Savioli L (2000) The global status of schistosomiasis and its control. *Acta Trop* **77**, 41–51.
5 Stothard JR, Chitsulo L, Kristensen TK & Utzinger J (2009) Control of schistosomiasis in sub-Saharan Africa: progress made, new opportunities and remaining challenges. *Parasitology* **136**, 1665–1675.
6 Fenwick A, Webster JP, Bosque-Oliva E, Blair L, Fleming FM, Zhang Y, Garba A, Stothard JR, Gabrielli AF, Clements AC *et al.* (2009) The Schistosomiasis Control Initiative (SCI): rationale, development and implementation from 2002–2008. *Parasitology* **136**, 1719–1730.
7 Fenwick A, Savioli L, Engels D, Bergquist RN & Todd MH (2003) Drugs for the control of parasitic diseases: current status and development in schistosomiasis. *Trends Parasitol* **19**, 509–515.
8 Ismail M, Botros S, Metwally A, William S, Farghally A, Tao LF, Day TA & Bennett JL (1999) Resistance to praziquantel: direct evidence from *Schistosoma mansoni* isolated from Egyptian villagers. *Am J Trop Med Hyg* **60**, 932–935.
9 Vermund SH, Bradley DJ & Ruiz-Tiben E (1983) Survival of *Schistosoma mansoni* in the human host: estimates from a community-based prospective study in Puerto Rico. *Am J Trop Med Hyg* **32**, 1040–1048.
10 Alger HM & Williams DL (2002) The disulfide redox system of *Schistosoma mansoni* and the importance of a multifunctional enzyme, thioredoxin glutathione reductase. *Mol Biochem Parasitol* **121**, 129–139.
11 Kuntz AN, Davioud-Charvet E, Sayed AA, Califf LL, Dessolin J, Arnér ES & Williams DL (2007) Thioredoxin glutathione reductase from *Schistosoma mansoni*: an essential parasite enzyme and a key drug target. *PLoS Med* **4**, e206.
12 Qiu J, Stevenson SH, O'Beirne MJ & Silverman RB (1999) 2,6-Difluorophenol as a bioisostere of a carboxylic acid: bioisosteric analogues of γ-aminobutyric acid. *J Med Chem* **42**, 329–332.
13 Biot C, Bauer H, Schirmer RH & Davioud-Charvet E (2004) 5-substituted tetrazoles as bioisosters of carboxylic acids. Bioisosterism and mechanistic studies on glutathione reductase inhibitors as antimalarials. *J Med Chem* **47**, 5972–5983.
14 Smart BE (2001) Fluorine substituent effects (on bioactivity). *J Fluorine Chem* **109**, 3–11.
15 Anderson JM & Kochi JK (1970) Silver (I)-catalyzed oxidative decarboxylation of acids by peroxydisulfate. Role of silver (II). *J Am Chem Soc* **92**, 1651–1659.
16 Feiring AE & Sheppard WA (1975) Fluorinated hydroquinones. *J Org Chem* **40**, 2543–2545.
17 Müller T, Johann L, Jannack B, Brückner M, Lanfranchi DA, Bauer H, Sanchez C, Yardley V, Deregnaucourt C, Schrével J *et al.* (2011) Glutathione reductase-catalyzed cascade of redox reactions to bioactivate potent antimalarial 1,4-naphthoquinones – a new strategy to combat malarial parasites. *J Am Chem Soc* **133**, 11557–11571.
18 Bauer B, Fritz-Wolf K, Winzer A, Kühner S, Little S, Yardley V, Vezin H, Palfey B, Schirmer RH & Davioud-Charvet E (2006) A fluoro analogue of the menadione derivative 6-[2′-(3′-methyl)-1′,4′-naphthoquinolyl]hexanoic acid is a suicide substrate of glutathione reductase. Crystal structure of the alkylated human enzyme. *J Am Chem Soc* **128**, 10784–10794.
19 Lanfranchi DA, Belorgey D, Müller T, Vezin H, Lanzer M & Davioud-Charvet E (2012) Exploring the trifluoromenadione core as template to design antimalarial redox-active agents interacting with glutathione reductase. *Org Biomol Chem* **10**, 4795–4806.
20 Kitz R & Wilson IB (1962) Esters of methanesulfonic acid as irreversible inhibitors of acetylcholinesterase. *J Biol Chem* **237**, 3245–3249.
21 Belorgey D, Lanfranchi DA & Davioud-Charvet E (2013) 1,4-Naphthoquinones and others NADPH-dependent glutathione reductase-catalyzed redox cyclers as antimalarial agents. *Curr Pharm Des* **19**, 2512–2528.
22 Morin C, Besset T, Moutet JC, Fayolle M, Brückner M, Limosin D, Becker K & Davioud-Charvet E (2008)

The aza-analogues of 1,4-naphthoquinones are potent substrates and inhibitors of plasmodial thioredoxin and glutathione reductases and of human erythrocyte glutathione reductase. *Org Biomol Chem* **6**, 2731–2742.
23 Amii H & Uneyama K (2009) C-F bond activation in organic synthesis. *Chem Rev* **109**, 2119–2183.
24 Mansuy D, Dansette PM, Pecquet F & Chottard JC (1980) Iron-porphyrin catalysis of the oxidative dealkylation of para-nitro-anisole and 7-ethoxycoumarin by cumylhydroperoxide: a possible model for the corresponding cytochrome P450-dependent reactions. *Biochem Biophys Res Commun* **96**, 433–439.
25 Oliveira MF, d'Avila JC, Torres CR, Oliveira PL, Tempone AJ, Rumjanek FD, Braga CM, Silva JR, Dansa-Petretski M, Oliveira MA, deSouza W & Ferreira ST (2000). Haemozoin in *Schistosoma mansoni*. *Mol Biochem Parasitol*, **11**, 217–221.
26 Thompson DC, Perera K & London R (2000) Spontaneous hydrolysis of 4-trifluoromethylphenol to a quinone methide and subsequent protein alkylation. *Chem Biol Interact* **126**, 1–14.
27 Sawyer DT, Sobkowiak A & Roberts JL (1995) Electrochemistry for Chemists, 2nd edn. John Wiley & Sons, New York, NY.
28 Nordhoff A, Bücheler US, Werner D & Schirmer RH (1993) Folding of the four domains and dimerization are impaired by the Gly446→Glu exchange in human glutathione reductase. Implications for the design of antiparasitic drugs. *Biochemistry* **32**, 4060–4066.
29 Gromer S, Merkle H, Schirmer RH & Becker K (2002) Human placenta thioredoxin reductase: preparation and inhibitor studies. *Methods Enzymol* **347**, 382–394.
30 Urig S, Fritz-Wolf K, Réau R, Herold-Mende C, Tóth K, Davioud-Charvet E & Becker K (2006) Undressing of phosphine gold (I) therapeutic agents as irreversible inhibitors of human disulfide reductases. *Angew Chem Int Ed Engl* **45**, 1881–1886.
31 O'Brien J, Wilson I, Orton T & Pognan F (2000) Investigation of the Alamar Blue (resazurin) fluorescent dye for the assessment of mammalian cell cytotoxicity. *Eur J Biochem* **267**, 5421–5426.
32 Lewis F (1998) Schistosomiasis. In *Current Protocols in Immunology* (Coligan JE, Kruisbeek AM, Margulies DH, Shevach EM & Strober W, eds), pp. 19–28. John Wiley & Sons, New York, NY.

Supporting information

Additional supporting information may be found in the online version of this article at the publisher's web site:

Fig. S1. Changes of the absorption spectra of the difluoromethylmenadione upon glutathione addition.

Fig. S2. Changes of the absorption spectra of the difluoromethyl derivative **8** upon glutathione addition.

Fig. S3. UV-Vis chromatograms and LC-MS traces after analysis of the glutathionylation reaction mixtures for difluoromethylmenadione–GSH conjugate formation.

Table S1. Proposed chemical structures of difluoromethylmenadione–glutathione adducts.

Table S2. IC_{50} values for 3-phenoxymethyl menadiones and their difluoromethymenadione derivatives in human lung MRC-5 fibroblasts *in vitro*.

Methods S1. Methods for LC-MS analysis of the difluoromethylmenadione–glutathione conjugates.